Automatic Viewpoint Selection for Exploration of Time-dependent Cerebral Aneurysm Data

Monique Meuschke[1], Wito Engelke[2], Oliver Beuing[3], Bernhard Preim[1], Kai Lawonn[4]

[1]Dept. of Computer Graphics and Simulation, OvG-University Magdeburg, Germany, and Research Campus STIMULATE
[2] Simulation and Software Technology, German Aerospace Center, Braunschweig, Germany
[3] Institute of Neuroradiology, University Hospital of Magdeburg, Germany, and Research Campus STIMULATE
[4] Institute of Computational Visualistics, University of Koblenz - Landau, Germany
`meuschke@isg.cs.uni-magdeburg.de`

Abstract. This paper presents an automatic selection of viewpoints, forming a camera path, to support the exploration of cerebral aneurysms. Aneurysms bear the risk of rupture with fatal consequences for the patient. For the rupture risk evaluation, a combined investigation of morphological and hemodynamic data is necessary. However, the extensive nature of the time-dependent data complicates the analysis. During exploration, domain experts have to manually determine appropriate views, which can be a tedious and time-consuming process. Our method determines optimal viewpoints automatically based on input data such as wall thickness or pressure. The viewpoint selection is modeled as an optimization problem. Our technique is applied to five data sets and we evaluate the results with two domain experts by conducting informal interviews.

1 Introduction

Cerebral aneurysms are abnormal dilatations of intracranial arteries, resulting from a pathological weakness in the vessel wall. Their rupture leads to a subarachnoid hemorrhage and is associated with a high mortality and morbidity rate. The aneurysm's initiation and outcome depends on different morphological and hemodynamic factors, whose impact on the individual rupture risk is not yet well understood. Computational Fluid Dynamic (CFD) simulations enable the investigation of the patient-specific internal wall mechanics and blood flow during the cardiac cycle. Experts are interested in correlations between hemodynamic factors that are associated with an increased risk of rupture. Therefore, hemodynamic and morphological parameters are visualized on the aneurysm surface simultaneously [1]. The problem of analyzing aneurysm data is twofold: first, the obtained flow data are very complex, and secondly, adjacent vessels could lead to occlusions. Domain experts have to manually search for suspicious regions by selecting views that enable an occlusion-free exploration. This can be

a tedious and time-consuming process. Therefore, a camera control including an adequate viewpoint selection is crucial for an efficient analysis.

There are several methods to determine good views for polygonal [2,3], volume data [4] and vector fields [5,6]. They mainly based on entropy [2], which is a measure to assess the quality of a view with the aim of maximizing its information content. For polygonal meshes, the relation between visible polygons and visible area [2] or surface parameters [3] were maximized. For volume data, voxel-based entropy functions were optimized and for vector fields, the visibility as well as flow parameters of streamlines were used. The suitability of a view also depends on application-specific characteristics, e.g., familiar and preferred views in surgery. Mühler et al. [7] integrated geometric aspects with such preferences.

In this work, we present an automatic calculation of a camera path to support the exploration of simulated aneurysm data. The camera path is composed of optimal viewpoints that present the most interesting regions during the cardiac cycle based on user-selected morphological and hemodynamic parameters. With our method, we enable the detection of suspicious surface regions without a time-consuming manual search. Our collaborating domain experts confirmed that our method supports the analysis of the time-dependent data.

2   Material and Methods

In this section, we describe the acquisition of simulated aneurysm data as well as our selection of appropriate viewpoints for the camera path.

2.1   Data Acquisition and Preprocessing

First, contrast-enhanced CT image data of the vessel morphology are acquired. Based on this, the vessel surface is reconstructed using the pipeline by Mönch et al. [8]. The 3D aneurysm surface and its parent vessel were extracted by using a threshold-based segmentation followed by a connected component analysis and Marching Cubes. The results are evaluated by medical experts to ensure anatomical plausibility. From the surface mesh, an unstructured volumetric grid is generated, on which a CFD simulation with a temporal resolution of 93 time steps is performed, using the STAR-CCM+ (CD-adapco, USA) solver.

2.2   Best Viewpoint Selection

This section explains our viewpoint selection. We describe the formulation of the target function, the start point sampling and the generation of the camera path.

Target Function: To select viewpoints, a target function $f : V \to \mathbb{R}$ has to be formulated that covers the criteria of an optimal viewpoint $\mathbf{x} \in V$. Selected viewpoints are local maxima of the target function that consists of two parts. The first one is the size of the visible aneurysm surface area, because mostly,

domain experts are interested in regions on the aneurysm. The second part is the significance of a surface area according to a user-selected parameter combination. For the first criteria, we separate the aneurysm from the parent vessel by segmenting it. This is done by an approach that determines the geodesic distance on the surface. For this, we place a start point on the aneurysm dome and compute the geodesic distance based on the heat equation [9]. Afterwards, we specify the distance that restricts the region of the aneurysm, including the ostium. For the second criteria, the user has to select two scalar parameters s_1 and s_2 that she wants to explore. Moreover, the user has to define if lower or higher values of the respective parameter should be weighted stronger. Based on the aneurysm segmentation, we implement a GPU-based approach to determine the target function's value for a specific viewpoint.

In the following, we explain how the target function $f(\mathbf{x})$ is defined for a viewpoint $\mathbf{x}$. Every fragment $p(\mathbf{x})$ in the current viewpoint $\mathbf{x}$ is assigned a value $t(p(\mathbf{x}))$. The sum of the fragment's values yields the target function $f(\mathbf{x}) = \sum_i t(p_i(\mathbf{x}))$. If the fragment p does neither belong to the segmentation nor to the front faces, we assign $t(p) = 0$. If $t(p)$ is not equal to zero, the two scalar values per fragment $s_1, s_2 \in [0,1]$ are multiplied by 10 and truncated to the nearest integer values, yielding $s_{i1}, s_{i2} \in \{0, \ldots, 10\}$. Moreover, s_{i1} and s_{i2} are squared to stronger weight interesting values. Additionally, we divide the framebuffer in $n \times n$ subimages and assign a constant factor $B_{ij} = \binom{n-1}{i} \cdot \binom{n-1}{j}$ to each subimage (i, j) in the design of a binomial filter. We used $n = 5$. Then, B_{ij} is added to s_{i1} and s_{i2}, depending on the subimage the current fragment belongs to, which yields the updated values s'_{i1} and s'_{i2}. This leads to a stronger weighting of s_{i1} and s_{i2}, if they occur in the center of the camera view. Lower values of n result in a too strong weighting of uninteresting surface regions, while higher values lead to an excessive weighting of small areas. We set $t(p) = s'_{i1} + s'_{i2}$, which represents the scalar value for a fragment p. Finally, we determine the target function $f(\mathbf{x})$ and store the value on an image, which allows a later CPU-based access.

After we used f to find appropriate starting points. The gradient ascent method is applied to each of them. The goal is to further optimize the two camera angles and the view direction (x, y, z), which results in five Degrees Of Freedom (DOF). Each DOF is changed iteratively, $f(\mathbf{x})$ is evaluated and the gradient of $f(\mathbf{x})$ is calculated. The new viewpoint $\mathbf{x}_{new}$ is calculated by $\mathbf{x}_{new} = \mathbf{x}_{old} + s \cdot \nabla f(\mathbf{x}_{old})$, where $\mathbf{x}_{old}$ is the current viewpoint, s is the step size and $\nabla f(\mathbf{x}_{old})$ is the gradient of $f(\mathbf{x}_{old})$. The gradient ascent stops if the gradient magnitude falls below a threshold t with $t = 0.001$. Moreover, f is evaluated for different values of s, where the integer values range from 1 to 5.

Starting point selection: The camera path should indicate interesting surface regions during the cardiac cycle. Within a time step, there are mostly several positions where significant parameter correlations arise. To find these local optima, we select multiple starting points per time step. It would be possible to define an arbitrary number of points at arbitrary positions around the aneurysm. However, possibly the optimization would require many iterations to find local optima.

Thus, we try to select starting points close to local optima on an approximated ellipsoid around the aneurysm. The ellipsoid's axes are the eigenvectors scaled by twice the eigenvalues of the covariance matrix of all aneurysm's vertices. The ellipsoid is sampled by using polar coordinates $\theta = 2\pi/36 \cdot i$, $i \in \{0, \ldots, 18\}$ and $\phi = 2\pi/m \cdot j$, with $m = 2 \cdot (9 - |i - 9|) + 1$, $j \in \{0, \ldots, m\}$. The scaling of the ellipsoid's eigenvalues ensures that the camera has an appropriate distance to the aneurysm, yielding the viewpoints $\mathbf{x}_i$. For each of these candidates, f is sampled. From this scalar field, we calculate the 90 % quantile and keep the remaining viewpoints as candidates for possible starting points. To further reduce their number, we cluster the candidates by using *DBSCAN*, a density-based clustering [10] that does not need a priori selection of the cluster number, because the number of optimal viewpoints is unknown. For each cluster, the averaged position is used as a starting point. However, for *DBSCAN* two thresholds must be specified, the minimum number of objects to form a valid cluster, and a maximum allowed dissimilarity between two objects of a cluster. In our case, each cluster must contain at least one candidate, and a maximum difference of 20 degrees for both angles, θ and ϕ, between a candidate and the cluster center is allowed. Smaller values lead to clusters, where the resulting starting points are very similar. With greater values the clusters are too large so that not all belonging candidates lie within the view frustum of the averaged camera position.

Camera animation: For each simulated time step, our approach calculates a set of optimal viewpoints. We order these viewpoints by their ϕ angle within a time step and connect them to a camera path. Moreover, the viewpoints are combined between adjacent time steps to generate a global camera animation during the cardiac cycle. Therefore, for each time step the viewpoint is used first that has the smallest distance of ϕ to the last viewpoint in the previous time step. We move the camera from one viewpoint in time to the next, where the camera position and view direction is interpolated from their known camera settings in each render pass. For the interpolation factor t, a cubic easing function is used with $t < .5 \; ? \; 4 \cdot t^3 : (t - 1) \cdot (2 \cdot t - 2) \cdot (2 \cdot t - 2) + 1$. With this the camera accelerates until halfway between two adjacent viewpoints and decelerates then. The resulting path enables a smooth animation between two adjacent viewpoints.

3   Results

We calculated camera animations for five data sets, where the results were evaluated with two domain experts by conducting informal interviews. The computation time per time step is between 8 and 10 s, depending on the amount of starting points. Our testing system uses an Intel Core i7 CPU with 2 GHz, 12 GB RAM and an NVidia GeForce GT 540M. The experts are one neuroradiologist with 16 years of work experience and one CFD engineer working on blood flow simulations for cerebral aneurysms with three years of work experience. They should assess if the automatic camera path supports the exploration and navigation within time-dependent data. Moreover, the experts had to manually search

for suspicious surface regions depending on the selected parameters s_1 and s_2. Fig. 1 shows the optimal viewpoints for two data sets at the systolic peak. The left part shows the segmented aneurysm together with the manually selected results of our neuroradiologist. In both cases, three optimal views (1,2,3) are detected, presented in the right part of the subimages. In Fig. 1(a) and (b) the Wall Shear Stress (WSS) and wall thickness are color-coded, respectively, and the wall deformation and pressure are depicted with illustrative techniques, respectively, as introduced in [1]. Reddish, dense hatched areas indicate suspicious surface regions. The experts described the camera path as very helpful for the exploration of the time-dependent data. The automatically selected views correlated with the manual results within that time step. However, for the manual searching a series of rotations was necessary. Further, the time-dependent behavior of the data increases the manual exploration effort, because it is difficult to find critical regions during animation, since the rotation process itself needs a certain amount of time. Moreover, the experts liked that no further specification of thresholds is necessary for the calculation of the camera path. In addition, they described the animation as helpful for the navigation in 3D. However, it depends on which part of the aneurysm the users want to navigate their way around. If the users only want to navigate in a small region such as a bleb, a manual rotation was preferred. For the time-dependent navigation over the whole aneurysm surface, the automatic rotation was preferred.
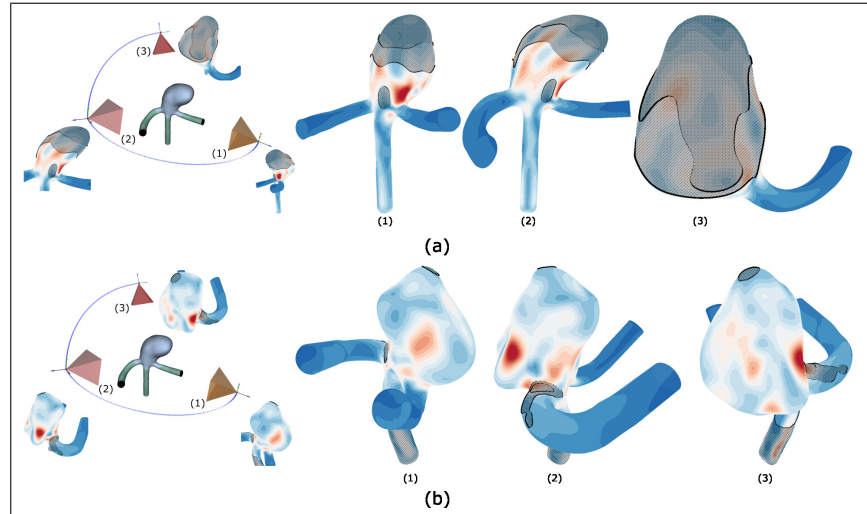
Fig. 1. Exemplary viewpoint selections for two data sets at the systolic peak. The left part shows the segmented aneurysm together with the manually selected results of our medical expert. For both, three optimal views (1,2,3) are detected, presented in the right part of the subimages. In (a) and (b), WSS and wall thickness are color-coded, respectively, and wall deformation and pressure are depicted by hatching, respectively. The camera is moving to all positions in a smooth way indicated by the purple spline.

4   Discussion

We present an automatic selection of occlusion-free views on suspicious surface regions for cerebral aneurysms based on user-selected parameters. From the viewpoints, a camera path is generated over the cardiac cycle. Our domain experts confirm the importance of camera paths to support the data exploration, because they enable the detection of suspicious regions without a time-consuming manual search. A possible application of our method is to get a quick overview of the aneurysm data, where rupture-prone areas are presented. In addition, our method could support the clinical report generation and serve as a summary of a patient's rupture risk. In the future, the camera path should be calculated in real time. Moreover, we want to integrate information about specific blood flow patterns such as vortices into the target function. Then, it would be possible to select views that present the time-dependent vortex behavior. A possible criterion in this context could be the optimization of the vortex core line visibility.

5   Acknowledgements

References

1. Meuschke M, Voss S, Beuing O, Preim B, Lawonn K. Combined Visualization of Vessel Deformation and Hemodynamics in Cerebral Aneurysms. IEEE Trans Vis Comput Graph. 2017;(01):761–70.
2. Vázquez PP, Feixas M, Sbert M, Heidrich W. Viewpoint selection using Viewpoint Entropy. In: Proc. of VMV; 2001. p. 273–80.
3. Neugebauer M, Lawonn K, Beuing O, Berg P, Janiga G, Preim B. AmniVis - A System for Qualitative Exploration of Near-Wall Hemodynamics in Cerebral Aneurysms. Comput Graph Forum. 2013;32(3):251–60.
4. Bordoloi UD, Shen HW. View selection for volume rendering. In: Proc. of the Conference on Visualization; 2005. p. 487–94.
5. Lee TY, Mishchenko O, Shen HW, Crawfis R. View point evaluation and streamline filtering for flow visualization. In: IEEE Pacific Vis Symposium; 2011. p. 83–90.
6. Tao J, Ma J, Wang C, Shene CK. A unified approach to streamline selection and viewpoint selection for 3D flow visualization. IEEE Trans Vis Comput Graph. 2013;19(3):393–406.
7. Mühler K, Neugebauer M, Tietjen C, Preim B. Viewpoint Selection for Intervention Planning. In: IEEE/Eurographics Symposium on Visualization; 2007. p. 267–74.
8. Mönch T, Neugebauer M, Preim B. Optimization of Vascular Surface Models for Computational Fluid Dynamics and Rapid Prototyping. In: Workshop on Digital Engineering; 2011. p. 16–23.
9. Crane K, Weischedel C, Wardetzky M. Geodesics in Heat: A New Approach to Computing Distance Based on Heat Flow. ACM Trans Graph. 2013;32.
10. Ester M, Kriegel HP, Sander J, Xu X. A density-based algorithm for discovering clusters in large spatial databases with noise. In: Proc. of Knowledge Discovery and Data Mining; 1996. p. 226–31.